Developmental Cell
Article

Hibris, a *Drosophila* Nephrin Homolog, Is Required for Presenilin-Mediated Notch and APP-like Cleavages

Jaskirat Singh[1] and Marek Mlodzik[1,*]
[1]Department of Developmental & Regenerative Biology, Mount Sinai School of Medicine and Graduate School of Biological Sciences, One Gustave L. Levy Place, Box 1020, New York, NY 10029, USA
*Correspondence: marek.mlodzik@mssm.edu
http://dx.doi.org/10.1016/j.devcel.2012.04.021

SUMMARY

Drosophila Hibris (Hbs), a member of the Nephrin Immunoglobulin Super Family, has been implicated in myogenesis and eye patterning. Here, we uncover a role of Hbs in Notch (N) signaling and γ-secretase processing. Loss of *hbs* results in classical N-signaling-associated phenotypes in *Drosophila*, including eye patterning, wing margin, and sensory organ specification defects. In particular, *hbs* mutant larvae display altered γ-secretase-dependent Notch proteolytic processing. Hbs also interacts molecularly and genetically with Presenilin (Psn) and other components of the γ-secretase complex. This Hbs function appears conserved, as mammalian Nephrin also promotes N signaling in mammalian cells. Our data suggest that Hbs is required for Psn maturation. Consistent with its role in Psn processing, Hbs genetically interacts with the *Drosophila* β-amyloid protein precursor-like (Appl) protein, the homolog of mammalian APP, the cleavage of which is associated with Alzheimer's disease. Thus, Hbs/Nephrin appear to share a general requirement in Psn/γ-secretase regulation and associated processes.

INTRODUCTION

Notch (N)-signaling is a conserved pathway and required in many processes during animal development and organ patterning (Artavanis-Tsakonas and Muskavitch, 2010; Fortini, 2009; Kopan and Ilagan, 2009) and has been extensively studied in *Drosophila* (Fortini, 2009). Signaling is initiated by the binding of the ligands Delta (Dl) or Serrate (Ser) to the transmembrane N receptor (Fehon et al., 1990). The ligand-receptor interaction stimulates extracellular cleavage of N by ADAM/TACE metalloproteases (Kuzbanian in *Drosophila*) (Hartmann et al., 2002; Pan and Rubin, 1997; Sotillos et al., 1997; Wen et al., 1997) and a subsequent intracellular cleavage close to the transmembrane domain by the gamma-secretase complex (Struhl and Greenwald, 1999), releasing the N intracellular domain (NICD or N^{intra}) (Schroeter et al., 1998; Struhl and Adachi, 1998). NICD can then transit to the nucleus to form a complex with the transcription factor Suppressor of Hairless Su(H)/CSL and activate gene transcription (Fortini and Artavanis-Tsakonas, 1994; Mumm and Kopan, 2000; Selkoe and Kopan, 2003).

Gamma-secretase is a multi-subunit protease complex that has been shown to cleave type I single-pass transmembrane proteins, including Amyloid Precursor protein (APP) and the N receptor. The complex itself consists of four proteins Presenilin, Nicastrin (Nct), APH-1 (anterior pharynx-defective 1), and PEN-2 (presenilin enhancer 2), with Psn acting as the catalytic subunit of the complex (De Strooper, 2003). Elimination of Presenilin1 in mammals leads to reduced γ-secretase-mediated cleavage of APP (De Strooper et al., 1998; Naruse et al., 1998). In mammals, biochemical studies have shown that Presenilin is synthesized as an immature holoprotein that undergoes endoproteolytic cleavage in one of the cytoplasmic loops that produces a larger N-terminal and a smaller C-terminal fragment, together forming the functional protein (Nowotny et al., 2000; Thinakaran et al., 1996). This endoproteolytic processing also requires Nct, APH-1, and PEN-2, which are required for proper Psn maturation (De Strooper, 2003; Hu and Fortini, 2003).

In *Drosophila*, N signaling is involved in almost every step of eye development, ranging from a role in growth control to lateral inhibition and cell fate specification of photoreceptors. In addition, it is required for correct planar cell polarity (PCP) specification in the eye (Mlodzik, 1999; Strutt and Strutt, 1999). PCP in the *Drosophila* eye is established by interplay between the Frizzled (Fz)/PCP and N signaling pathways in third instar larval eye discs, leading to correct specification of the photoreceptor R3 and R4 precursors (Cooper and Bray, 1999; Fanto and Mlodzik, 1999; Tomlinson and Struhl, 1999). At the five-cell precluster stage, the R3 precursor, which is closer to the D/V-midline, sees higher levels of Fz/PCP signaling (Tomlinson and Struhl, 1999; Zheng et al., 1995) and adopts the R3 fate. Fz activity then activates *Dl* transcription in R3, which in turn signals to N in the adjacent cell, specifying it as R4 (Cooper and Bray, 1999; Fanto and Mlodzik, 1999). Thus, N signaling acts downstream of Fz/PCP signaling to control PCP-mediated cell fate specification in the eye.

In a search for molecules involved in PCP regulation in the *Drosophila* eye, we have identified the Immunoglobulin Super Family (IgSF) member *hibris* (*hbs*, J.S. and M.M., unpublished data). Hbs is a transmembrane protein with multiple extracellular Ig-repeats and is homologous to vertebrate Nephrins (Dworak et al., 2001; Artero et al., 2001). It is expressed dynamically during all developmental stages (Dworak et al., 2001) and can

interact across cell membranes with the related Roughest (Rst) and Kirre proteins, members of the Neph family of adhesion factors (Bao and Cagan, 2005). This cell adhesion function of Hbs has been implicated in embryonic myogenesis and late pupal eye patterning (Artero et al., 2001; Bao and Cagan, 2005; Dworak et al., 2001). Recently it has also been suggested that *hbs* acts in PCP establishment through its genetic interaction with Mtl, a member of the Rho GTPase subfamily (Muñoz-Soriano et al., 2011), though the mechanism or mechanisms by which Hbs might influence PCP have not been addressed.

In this study we have uncovered a role of the IgSF member Hbs in N and Appl signaling via Psn processing. Hbs loss gives classical N loss-of-function phenotypes, including cell fate specification and PCP-associated defects in the eye, wing margin defects, and sensory organ specification defects. Hbs acts as a positive regulator of N signaling. Loss of *hbs* suppresses phenotypes caused by expression of membrane-tethered active Notch but not a constitutively active intracellular form of Notch (N^{intra}), suggesting defects in Notch activation downstream of ligand binding. Consistently, *hbs* mutant larvae display altered Notch protein cleavage/processing. Importantly, *hbs* genetically and molecularly also interacts with Presenilin (Psn) and Nicastrin (Nct), components of the γ-secretase complex. Strikingly, Hbs is required for Psn maturation. Consistent with these findings *hbs* genetically also interacts with *Drosophila* APPL, the homolog of mammalian APP, a well-known Psn substrate in the context of Alzheimer's disease. The mammalian Hbs ortholog, Nephrin, also promotes Notch-signaling in mammalian cells, and thus this function of Hbs/Nephrin likely represents a conserved requirement in Psn-associated processes.

RESULTS

Hbs Loss and Gain of Function Cause PCP Phenotypes in the Eye

To determine a specific role of Hbs in eye PCP specification, we expressed *UAS-hbs^{RNAi}* (*hbs-IR*) using *sevenless-Gal4* (*sevGal4*), which drives expression in the R3/R4 precursors during PCP establishment (and later also in R1/R6 and R7). Fz/PCP-signaling activity in R3 precursors leads to the upregulation of *Dl* and *neuralized* expression, which in turn activates N signaling in the adjacent cell, specifying it as R4 (Cooper and Bray, 1999; del Alamo and Mlodzik, 2006; Fanto and Mlodzik, 1999; Tomlinson and Struhl, 1999). If this interplay is disrupted by mutations in components of either the Fz/PCP or N pathways, either the R3-R4 cell fate decision is randomized or both precursors adopt the R3 fate (when Fz-signaling is increased or N signaling is reduced) or the R4 fate (when N signaling is activated in both precursors; Cooper and Bray, 1999; del Alamo and Mlodzik, 2006; Fanto and Mlodzik, 1999; Tomlinson and Struhl, 1999). Eyes of *sevGal4, UAS-hbs-IR* flies displayed dosage-dependent PCP defects manifest as symmetrical clusters of the R3-R3 type, ommatidial rotation defects, and occasional loss of photoreceptors (Figures 1A–1C and Table 1). Removal of a genomic copy of *hbs* (*hbs$^{459/+}$*) enhanced the *hbs-IR* phenotypes, confirming its specificity (Figures 1B–1C). As Gal4 activity is temperature dependent, expression of *hbs-IR* at higher temperature (29°C) resulted in stronger PCP defects (Figure 1D). Although several *hbs* alleles have been reported, none of them are protein null (Figures S1D, S1D', and S1D'', available online). We thus generated a new strong *hbs* allele (hereafter *hbs^{J5}*) by excising the genomic region between two *piggyBac/FRT* insertions (see Experimental Procedures for details). All *hbs* alleles (*hbs^{J5}*, *hbs^{J5}*/Df(2R)ED2423, and the previously reported *hbs^{459}*) produced similar eye phenotypes as *hbs-IR* (Figures 1E, Table 1, and Figure S1A; data not shown). We confirmed with an antibody to Hbs that *hbs-IR* eliminates Hbs protein expression (*engrailedGal4 > hbs-IR*; Figures S2A–S2A'), indicating that *hbs-IR* mimics a strong LOF allele. Clones of another *hbs* allele (*hbs^{EP}*) also displayed similar eye defects (Figure S1B). We next analyzed whether Hbs overexpression could affect R3/R4 cell fate specification, as PCP factors generally affect the process in both loss- and gain-of-function scenarios (Boutros et al., 1998; Tomlinson and Struhl, 1999). Expression of Hbs (*UAS-Hbs,* under *sevGal4* control) resulted in classical eye PCP defects (including chirality and ommatidial rotation defects) and also some R-cell loss (Figure 1F and Table 1). The gain-of-function phenotypes were stronger at 29°C with many symmetrical clusters and an increase in photoreceptor loss (Table 1 and Figure S1C). Taken together, these data suggest that Hbs is involved in establishing PCP in the eye and also in specification or differentiation of other R-cells.

Hbs Is Expressed in Developing R-Cell Preclusters with Membrane and Vesicular Localization

Consistent with a role in eye PCP establishment and R-cell specification, *hbs* expression is upregulated in the morphogenetic furrow (MF; arrow in Figures 2A–2A'') and in developing clusters as they emerge as arcs from the MF (in addition to a lower level ubiquitous expression in all cells). Subsequently, by row 2–4 Hbs expression was enriched around ommatidial preclusters and was also detected in all developing photoreceptors (including R3/R4) at the time of PCP establishment (arrowheads in Figure 2A''). This expression pattern is consistent with the notion that Hbs is required in the R3/R4 specification context and/or other photoreceptor cell fate decisions. Hbs expression is maintained at later stages of eye development, consistent with its reported role in pupal eye patterning (Bao and Cagan, 2005). Intriguingly, besides its membrane association, we also consistently detected a significant portion of Hbs in intracellular puncta in imaginal discs (Figures 2B–2B'' and 2D–D'', when imaged at a more basal plane; see also x/z-sections in Figures 2C–2C'). To determine the nature of the Hbs-positive intracellular puncta, we costained eye discs with vesicular markers. Most Hbs puncta colocalized with Rab5, a marker for early endosomes (Figures 2D–2E, also x/z-section in Figures 2F–2F''). Some colocalization was also seen with Rab11-positive vesicles (recycling endosomes), whereas in contrast no colocalization was seen with Rab7 (Figures 2G–2G'' and Figures 2H–2H''). These data suggest that Hbs not only gets enriched apically at plasma membranes near junctions but is also present in early and recycling endosomes.

Loss of *hbs* Mimics *Notch* Loss-of-Function Phenotypes in Several Tissues

To define the role of Hbs in eye PCP specification and to establish whether it acts in Fz/PCP or N signaling, we tested the N-signaling reporter *mδ0.5,* a 500-base-pair fragment of the

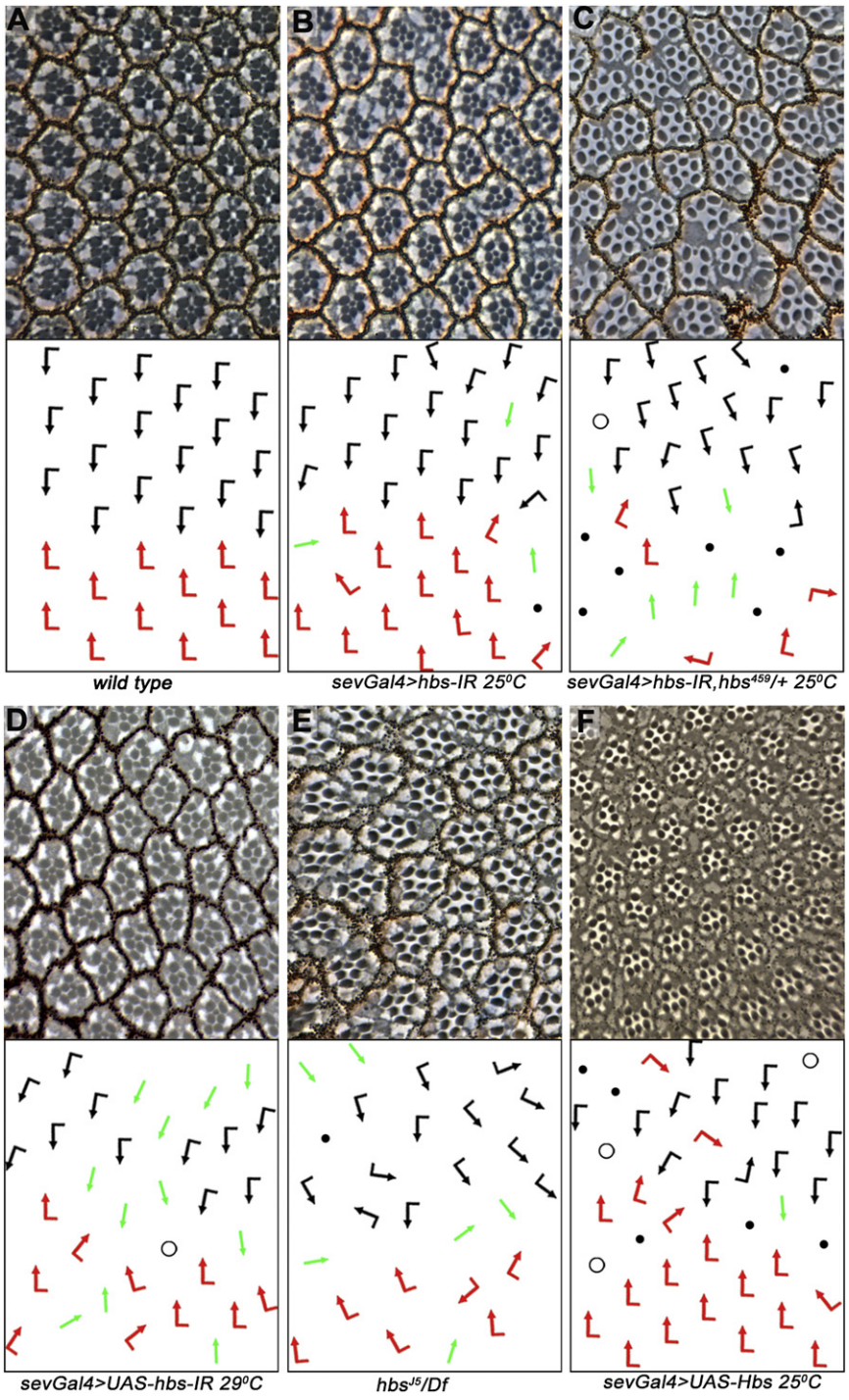

Figure 1. *hbs* Loss and Gain of Function Displays PCP Eye Phenotypes

(A–F) Tangential eye sections of adult eyes of indicated genotypes, centered around the D/V-midline or equator. (Bottom) Schematic representations of ommatidial polarity. Anterior is left and dorsal up in all panels. Black and red arrows represent dorsal and ventral chiral forms, respectively; green arrows represent R3-R3 symmetrical clusters; open circles represent ommatidia with loss of R7; and black dots represent ommatidia with a reduced number of R-cells. (A) Wild-type: regular ommatidial arrangement of opposing chiralities forming a mirror image across the equator. (B) *sevGal4*, *UAS-hbs-IR* at 25°C. Note symmetrical clusters (green arrows), rotation defects, and some loss of R-cells. (C) *sevGal4*, *UAS-hbs-IR* is enhanced by *hbs* heterozygosity (*sev > hbs-IR; hbs*^{459}/+), confirming specificity of RNAi. (E) *hbs*^{459}/Df(2R)ED2423: note PCP defects and R-cell loss comparable to the *hbs-RNAi* experiments (B–D) quantified in Table 1. (F) Overexpression of Hbs using *sevGal4* (*sevGal4, UAS-Hbs*) causes similar eye phenotypes (compare to C–E). See also Figure S1.

E(spl)mδ promoter (Cooper and Bray, 1999), which serves as a marker for R4 specification and a molecular readout of N activity (*mδ0.5* is first expressed at low levels in both R3/R4 cells and then upregulated specifically in R4 in response to N-activation). Strikingly, expression of *mδ0.5Gal4, UAS-GFP* (*mδ0.5 > GFP*) was reduced or lost in *hbs* mutant clones in third instar discs (Figure 3A, arrowheads), suggesting defects in N signaling and R4 cell fate specification. To determine whether *hbs* is generally required for N signaling, we tested its functions in other tissues patterned by N signaling. In the wing, N signaling is required, among others, for the formation of the dorsal/ventral (D/V) compartment boundary and wing margin specification, and loss-of-function *N* alleles cause wing notching phenotypes (de Celis et al., 1996; Shellenbarger and Mohler, 1978). We tested whether *hbs* has a role in modulating N signaling in this context. Expression of *enGal4 > hbs-IR* (expressed in the posterior compartment [P], highlighted in Figure 3B) resulted in wing notching phenotypes reminiscent of N signaling defects (Figure 3C; wing notching phenotypes were also seen in clones of two *hbs* alleles, Figures S3A–S3B). Consistently, *en > hbs-IR* resulted in reduced expression of the N-signaling target gene *cut* at the prospective posterior wing margin (Figures 3D–3D'', anterior compartment [marked by Ci in red] acts as internal control as *hbs-IR* is not expressed there). Of note, overexpression of Hbs (*enGal4 > UAS-Hbs*) also resulted in wing notching phenotypes and reduction of Cut expression in the posterior compartment, suggesting that too much Hbs acts as dominant negative (Figures S3C, S3D, and S3E, see Discussion for details).

Asymmetric activation of N signaling in sensory organ precursor cells is required for proper development of thoracic sensory bristles, consisting of shaft, socket, sheath, and neuronal cells (Figure 3E). Failure of N signaling during sensory

Table 1. Quantification of Phenotypes and Genetic Interactions

Genotype	Wild-Type	Chirality Defects	Rotation Defects	Not Scorable
sevGal4 > hbs-IR 25°C	77.7 ± 2.2	3.0 ± 1.3	16.4 ± 1.1	2.9 ± 0.1
sevGal4 > hbs-IR, hbs^{459}/+ 25°C	60.5 ± 5.7	11.7 ± 2.2	16.6 ± 1.1	12.5 ± 1.4
sevGal4 > hbs-IR 29°C	56.9 ± 5.9	19.4 ± 2.3	14.0 ± 2.4	9.7 ± 6.9
sevGal4 > UAS-Hbs 25°C	60.4 ± 3.0	2.9 ± 1.8	5.6 ± 2.7	31.1 ± 3.8
sevGal4 > UAS-Hbs 29°C	24.3 ± 6.9	7.4 ± 1.5	9.6 ± 1.9	60.5 ± 9.1
hbs^{J5}/*Df(2R)ED2423*	51.0 ± 11.7	11.0 ± 3.6	29.9 ± 10.2	8.2 ± 1.5
N^{55e11}/+; *sevGal4 > hbs-IR* 25°C	80.2 ± 7.9	12.9 ± 3.1	6.6 ± 5.6	0.9 ± 1.6
$sevN^{\Delta ECD}$ 29°C	35.9 ± 0.5	32.5 ± 5.5	–	43.7 ± 10.3
$sevN^{\Delta ECD}$, *sevGal4 > hbs-IR* 29°C	23.7 ± 6.1	9.4 ± 4.1	–	54.6 ± 4.3
sevGal4 > hbs-IR, kuz^{e29-4}/+ 25°C	81.5 ± 8.2	4.3 ± 1.3	12.4 ± 6.7	1.7 ± 1.9
sevGal4 > hbs-IR, psn^{143}/+ 25°C	53.9 ± 3.4	19.6 ± 1.0	19.1 ± 3.8	7.4 ± 3.4
sevGal4 > hbs-IR, psn^{9}/+ 25°C	63.7 ± 2.5	11.8 ± 1.1	18.8 ± 2.4	5.7 ± 1.7
sevGal4 > hbs-IR, *psn-IR*/+ 25°C	64.4 ± 4.2	14.3 ± 1.3	13.5 ± 3.2	7.8 ± 4.0
sevGal4 > hbs-IR, nct^{A7}/+ 25°C	83.2 ± 2.7	12.1 ± 2.8	–	4.8 ± 1.2
sevGal4 > appl-IR 25°C	33.5 ± 8.7	7.9 ± 4.2	–	59.0 ± 5.2
sevGal4 > hbs-IR, *appl-IR* 25°C	22.1 ± 5.7	34.6 ± 5.0	–	43.3 ± 8.2

For each genotype at least three independent eyes were scored and more than 300 ommatidia were counted. Numbers represent percentages of ommatidia ± standard deviation. Unscorable clusters consist of fewer or more than the normal R-cell complement, and thus their orientation cannot be scored.

bristle group development results in all cells adopting a neuronal fate at the expense of the accessory fates (Figure 3E'; Lai and Orgogozo, 2004). Because higher levels of Hbs are expressed in the developing sensory bristle clusters (as compared to surrounding epithelial cells; Figures S2B–S2B''), we tested whether *hbs* mutants display bristle group phenotypes. In wild-type, a regular pattern of bristles was observed (Figure 3F), whereas *hbs* mutants (hbs^{J5}/*Df(2R)ED2423* and hbs^{459}/*Df(2R)ED2423*) displayed a reduction in bristle numbers (Figures 3H and S3H). To test whether this is due to aberrant N-signaling-mediated cell fate specification within the SOP group, we analyzed their development at 24 hr APF with the neuronal marker Elav and Cut (marking all cells of the SOP cluster). In wild-type, each Cut-expressing cluster includes a single Elav-expressing neuron (Figure 3G). In contrast, in *hbs* mutants most SOP clusters displayed several Elav-positive cells (Figure 3I), implying defects in N signaling. Similar to *hbs* mutants, loss of external bristle structures was also observed when *hbs-IR* was expressed under *pannier-gal4* control (expressed centrally in the developing thorax; Figures S3F–S3G). These phenotypes suggest a general requirement in N signaling.

To further address the role of *hbs* in N signaling, we tested whether reduction in N levels can modify *hbs* LOF phenotypes. In the eye, removing one copy of *N* (N^{55e11}/+, which by itself has no eye phenotype, data not shown) strongly enhanced the *sevGal4 > hbs-IR* phenotypes (Figures 4A–4C; Table 1). Specifically, N^{55e11}/+, *sevGal4 > hbs-IR* displayed a marked increase in R3-R3 symmetrical clusters (compared to *sevGal4 > hbs-IR* alone), consistent with a reduction in N-dependent R4 specification. In the thorax, reducing *N* dosage resulted in an enhancement of the hbs^{J5}/*Df(2R)ED2423*-associated bristle loss phenotype (Figures 4D–4F; N^{-}/+ has no thorax phenotype alone). Similar interactions were also observed between several *N* and other *hbs* alleles (Figures S3H–S3I). Taken together, these data confirmed a role of *hbs* in N signaling.

Strikingly, in addition to these N-signaling phenotypes, *hbs* expression is upregulated in most contexts in which high levels N signaling are required. Besides the MF and R-cell preclusters in the eye (Figure 2), Hbs is also expressed at high levels at the wing margin (Figures S2A and S2C–S2F'') and within the SOP groups (Figures S2B–S2B''). Interestingly, these expression patterns are under the control of several signaling pathways, including Wg-signaling in the wing or Egfr/Ras-signaling in the eye (Figure S2 and data not shown), which could thus affect N-signaling levels (see Discussion). In summary, the phenotypic data, genetic interactions, and expression in imaginal discs are all consistent with the notion that *hbs* is generally required for (and possibly a component of) N signaling.

hbs Is Required for the Activity of Membrane-Tethered Notch but Not for $Notch^{intra}$ In Vivo

To address molecular mechanism(s) of how Hbs could affect N signaling, we first tested the effect of Hbs on an N-responsive reporter (NRE) (Bray et al., 2005). Full-length N-mediated induction of the NRE in S2 cells was potentiated in a dosage-dependent manner by Hbs coexpression (Figure 5A). In contrast, cotransfection of Hbs did not affect the level of NRE activation by the constitutively active cytoplasmic fragment of N (N^{intra}; Figure 5B). As N^{intra} acts independently of upstream regulation, this result suggested that Hbs is required for activation of membrane-tethered N, or related membrane-associated processes, rather than downstream signaling events.

Hbs encodes a transmembrane IgSF protein and shares extensive homology to mammalian Nephrins. Nephrins are expressed in diverse organisms ranging from worms to mammals (Dworak et al., 2001). In vertebrates, Nephrin has been studied

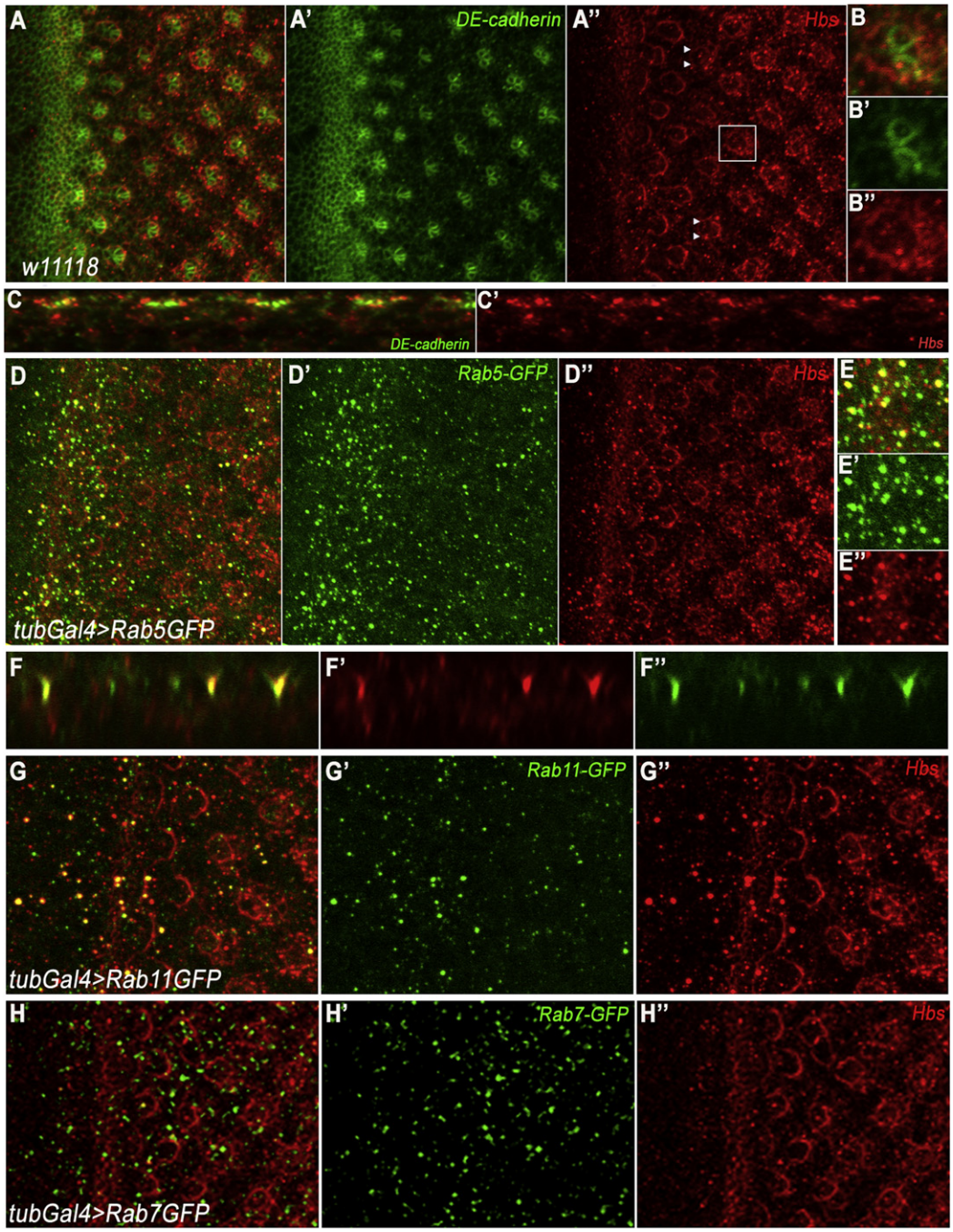

Figure 2. Hbs Is Localized at Membranes/Junctions and in Intracellular Puncta

(A and B) Confocal projections depicting localization of Hbs (red) and DE-cadherin (green, marking cellular outlines at junctional level and highlighting developing photoreceptor clusters) in third instar eye discs. Hbs is upregulated in the furrow (MF, white arrow in A and A'') and R-cell preclusters as they emerge from MF. Hbs is enriched at membranes surrounding ommatidial preclusters (A'', magnified in B–B''), reflecting expression in all R-cells.

(C and C') x/z-section of third instar eye disc in (A). Note that Hbs is not only enriched in junctional membranes but is also present in intracellular puncta throughout R cells.

(D and E) x/y-section of third instar eye disc of *tubGal4 > Rab5GFP* genotype, stained for Hbs (red) and Rab5GFP (green). Note Hbs-positive puncta colocalize (magnified in E–E') with Rab5GFP puncta, a marker for early endosomes.

(F and F') x/z-section of third instar eye disc in (D), showing colocalization of Hbs and Rab5 positive puncta in yellow in (F).

(G and G') *tubGal4 > Rab11GFP* eye discs showing colocalization of Hbs (red) with recycling endosomal marker Rab11 (green).

(H and H') *tubGal4 > Rab7GFP* eye discs showing expression of Hbs (red) and Rab7GFP (green). Hbs does not colocalize with late endosomal marker Rab7 (green).

See also Figure S2.

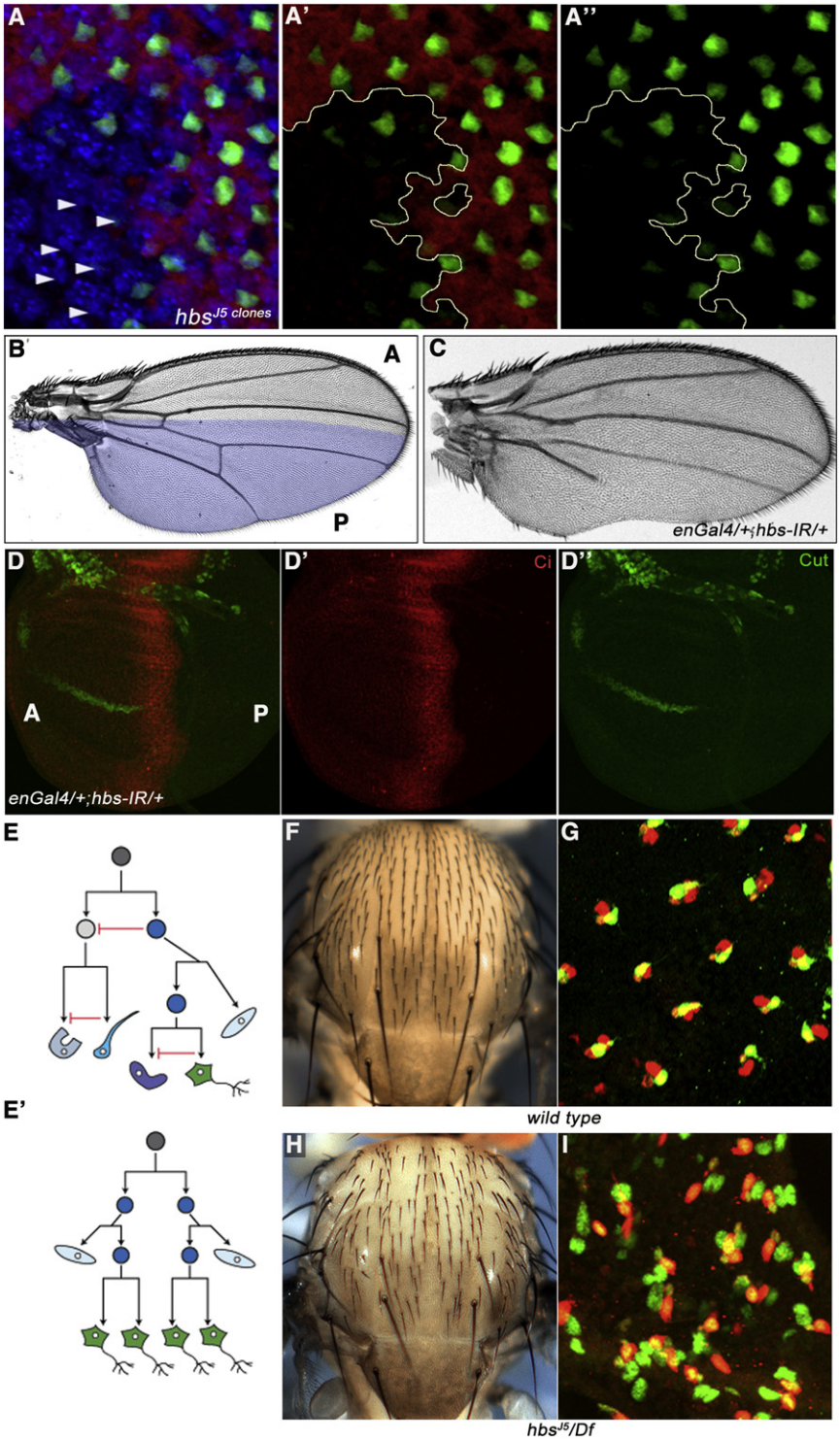

Figure 3. *hbs* Loss of Function Resembles N-Signaling Loss-of-Function Defects

(A–A'') Confocal projections of third instar eye discs stained for $m\delta^{0.5}$*Gal4* > *GFP* (green; N-signaling reporter in R4), neuronal marker Elav (blue, labeling all R-cells), and lacZ (red, labeling wild-type tissue), *hbs* mutant tissue (marked by absence of red) is outlined by yellow lines in (A'–A''). $m\delta^{0.5}$*Gal4* > *GFP* expression is reduced or often lost in preclusters mutant for *hbs*, suggesting a failure of N-signaling target activation in R4 cells.

(B and C) Adult wings. (B) Wild-type wing with highlighted *engrailed (en)* expression domain in posterior compartment (P). (C) *enGal4, UAS-hbs-IR (enGal4 > hbs-IR,* at 29°C) results in wing notching and vein formation defects.

(D–D'') Confocal projections of *enGal4, UAS-hbs-IR* third instar wing disc stained for the N-signaling target Cut (green) and Ci (red, marking anterior compartment [A]). Cut expression is lost/reduced in P compartment. *en*-expression expands into the A compartment at this stage, and hence Cut expression is also affected near the border in the A compartment.

(E and E') Schematic of divisions within a sensory organ, consisting of two external cells, shaft and socket, and two internal cells, neuron (green) and sheath (glia-like), which arise from a series of asymmetric divisions from a single sensory organ precursor (SOP) cell. Directional Delta/N signaling specifies the two daughter cells to adopt different fates. Red inhibitory arrow represents N signaling in (E). In *N* loss of function (E') all four cells are specified as neurons (green), leading to loss of external bristles.

(F and G) Wild-type adult thorax showing mechanosensory bristles, patterned uniformly across the notum (F) and (G) confocal projections of anterior notum at 24–28 hr APF, stained for Elav (green; neuronal marker) and Cut (red; labeling all SOP cluster cells). Note: each cluster has only one Elav-positive cell.

(H and I) *hbs* mutant thorax (*hbs*^{J5}*/Df(2R)ED2423*) showing bald patches as a result of missing bristle cells in adults (H), and confocal projections of equivalent notum at 24–28 hr APF (I) with multiple Elav-positive (green) cells per SOP cluster, suggesting failure of N-signaling-based cell fate specification in *hbs* mutants.

See also Figure S3.

mostly in the context of the slit diaphragm, a specialized junction in the kidney glomerulus, which is involved in filtering blood (Holzman et al., 1999; Ruotsalainen et al., 1999). We next tested whether the N-signaling-related function of Hbs/Nephrin is conserved in mammals and asked whether Nephrin can potentiate N signaling in mammalian cells. We coexpressed mTM-Notch1 (a mouse Notch1 isoform, inserted in the membrane, that requires the final [S3] cleavage for activation) along with Nephrin in the presence of a Notch reporter. mTM-Notch1 expression alone resulted in induction of the reporter as expected (Figure 5C). Strikingly, coexpression of Nephrin along with mTM-Notch1 caused a dosage-dependent increase in N-reporter activity (Figure 5C). Consistent with the *Drosophila* data, expression of Nephrin did not modify the level of N reporter activity induced by mNotch1^{intra} (Figure 5D). Taken together, the role

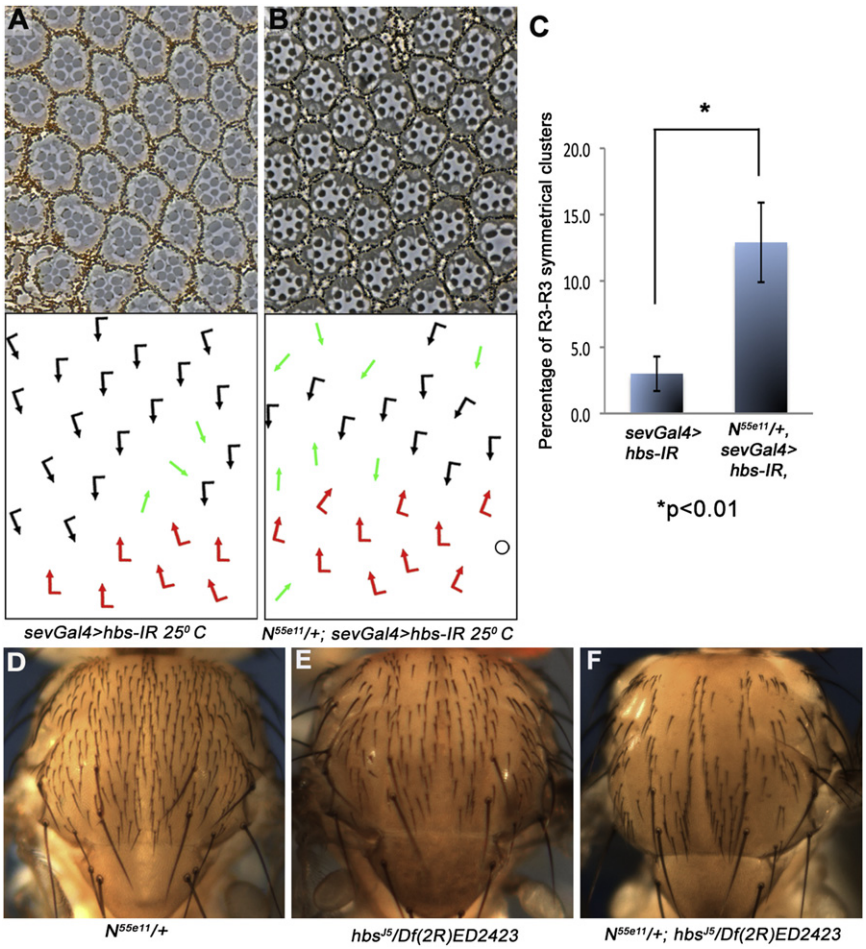

Figure 4. *hbs* Genetically Interacts with *N*

(A–C) Tangential eye sections of adult eyes of indicated genotypes (at 25°C; centered around the equator); bottom panels show schematic representations of ommatidial polarity. Anterior is left and dorsal is up. (A) *sevGal4*, *UAS-hbs-IR* and (B) N^{-}/+; *sevGal4*, *UAS-hbs-IR*: The N^{55e11}/+ background enhances the *hbs-IR* phenotype, most evident in the increase in R3-R3 symmetrical clusters, quantified in (C); graph shows mean ± standard deviation (SD) of three eyes, n > 300 ommatidia scored, p value: *p < 0.01 (as determined by Student's t test).

(D–F) Dorsal thorax view of indicated genotypes, anterior is up. (D) N^{55e11}/+ thorax (control) showing normal sensory bristles arrangement, (E) hbs^{J5}/*Df(2R)ED2423* thorax with some missing bristles, and (F) N^{55e11}/+; hbs^{J5}/*Df(2R)ED2423* thorax. Note strong enhancement of the hbs^{J5}/*Df(2R)ED2423* phenotype by removing a copy of *N*.

of Hbs and Nephrin in regulating membrane-associated events in N signaling appears conserved.

To corroborate this hypothesis in vivo, we tested the requirement of Hbs for N-signaling activity in the *Drosophila* eye. Expression of a truncated membrane-tethered form of N ($N^{\Delta ECD}$) that lacks most of the extracellular domain and functions in a ligand-independent manner (Fortini et al., 1993), resulted in frequent R4-R4 symmetrical clusters (*sev-*$N^{\Delta ECD}$; with 32.6% ± 5.5% R4-R4 clusters, Figure 5E, Table 1, and Figure S4A) and frequent transformations of outer R1/R6 to inner R7s as reported (Fortini et al., 1993; Tomlinson and Struhl, 1999). The number of R4-R4 clusters was markedly reduced by coexpression of *hbs-IR* in *sev-*$N^{\Delta ECD}$ eyes (Figures 5E–5F, quantified in Table 1 and Figure S4A). Notably, even R3-R3 symmetrical clusters, never seen in a *sev-*$N^{\Delta ECD}$ background, were observed in *sevGal4* > *hbs-IR, sev-*$N^{\Delta ECD}$, suggesting repression of N activity. Similar suppression of *sev-*$N^{\Delta ECD}$ was seen when we removed a genomic copy of *hbs* (data not shown). In contrast to the membrane-tethered $N^{\Delta ECD}$, the equivalent eye phenotypes of the soluble N^{intra} isoform (Tomlinson and Struhl, 1999) were not affected by *hbs-IR* (Figures 5G–5H; *sev-*N^{intra} and *sevGal4* > *hbs-IR, sev-*N^{intra} displayed indistinguishable phenotypes; also Table 1). Taken together, these data are consistent with a positive requirement of Hbs in N signaling. Importantly, our data indicated that Hbs was required for activation of trans-membrane N proteins but is dispensable for shorter soluble isoforms, not requiring membrane-associated cleavage. Hence, we tested whether Hbs affected cleavage of Notch. Western analysis of *hbs* mutant eye/brain complexes revealed an altered banding pattern of N, with the levels of the fully cleaved low molecular bands (equivalent to N^{intra}, ~120 kDa fragment) markedly reduced (Figure 5I, black arrow; quantified in Figure 5I'). Similar reduction in $Notch^{intra}$ levels were observed in *hbsIR* wing discs under *nubGal4*-driven expression (expressed in all wing blade cells, Figure S4B).

Loss of *hbs* Affects the Psn/γ-Secretase-Mediated Notch Cleavage Pattern

The Notch receptor undergoes a ligand-dependent cleavage mediated by the Kuzbanian/TACE metalloproteases at an extracellular site close to the membrane (Pan and Rubin, 1997; Sotillos et al., 1997; Wen et al., 1997). Subsequently, Notch undergoes an intra-membranous cleavage mediated by the γ-secretase complex consisting of Psn, Nct, Aph-1, and Pen-2 (De Strooper et al., 1999; Ray et al., 1999; Struhl and Greenwald, 1999; Ye and Fortini, 1998). The $N^{\Delta ECD}$ construct represents an isoform of N that does not require the extracellular TACE/Kuzbanian-mediated (S2) cleavage for activation. Because the activity of $N^{\Delta ECD}$ (which does not require Kuz-mediated S2 cleavage) was suppressed by reducing *hbs* levels (*hbs-IR*, Figure 5F), this would suggest that Hbs functions downstream of TACE/Kuz. Accordingly, reduction of Kuz levels (kuz^{-}/+) in *hbs-IR* backgrounds had no detectable effect on *hbs-IR* eye phenotypes (Figures 6A–6B, quantified in Figure 6E and Table 1). We next tested whether Hbs has a role in Psn-mediated cleavage of N (Struhl and Greenwald, 1999). Strikingly, removing a genomic copy of *psn* (via either the psn^{143} or psn^{9} alleles)

resulted in a dominant enhancement of the frequency of R3-R3 symmetrical clusters induced by *sev > hbs-IR* (Figures 6C–6D and Table 1). Similarly, expression of *psn-IR* in the eye enhanced the *sev > hbs-IR* PCP phenotype (Figures S5A–S5B). Removing a genomic copy of *psn* (psn^{143}/+) enhanced the *sevGal4 > UAS-Hbs* PCP phenotype, consistent with the notion that overexpression of Hbs in vivo acts as a dominant negative (Table 1 and Figures S5C–S5D, also Discussion). Importantly, *psn* also enhanced the effects of *hbs* mutants in other tissues. For example, the hypomorphic psn^{143}/psn^{9} *trans*-heterozygous background, which displayed no thoracic abnormalities by itself (Figure 6F), strongly enhanced the bristle loss of hbs^{J5}/ *Df(2R) ED2423* and hbs^{459}/ *Df(2R)ED2423* mutants (Figures 6F–6H and data not shown). Of note, removing a genomic copy of *nct* (nct^{A7}/+), another component of γ-secretase, also enhanced *hbs-IR* PCP phenotypes (Figures 6D–6E and Table 1), suggesting a role of Hbs in γ-secretase complex function.

Next we investigated whether the genetic *hbs-psn* interactions were supported by a molecular association. First, we observed Hbs and Psn colocalization in S2 cells (Figures S5E–S5E''; both proteins localizing to the same subcellular compartments). Colocalization was confirmed in third instar imaginal discs at endogenous levels: PsnHA (a biologically active, HA-epitope-tagged, form of Psn [Chung and Struhl, 2001]) and endogenous Hbs colocalized to the same subcellular compartments (Figures S5F–S5H''). Similar colocalization of PsnHA and Hbs was also detected in developing wing discs (Figures S5H–S5H''). Second, we tested whether Hbs can physically associate with Psn. Hbs-HA (haemagglutinin-tag) was transfected alone or together with Psn-Myc, Fz-Myc, and/or DE-cadherin (Fz-Myc and DE-cadherin act as negative controls to rule out nonspecific binding of Hbs-HA and Psn-Myc to other trans-membrane proteins). Immunoprecipitation of Psn-Myc specifically coimmonoprecipitated Hbs-HA (Figure 6I), whereas DE-cadherin (Figure 6I) and Fz-Myc did not pull down Hbs-HA (Figure S5I), indicating a specific molecular interaction between Hbs and Psn. Of note, very similar physical interactions were also observed between Hbs and Nct in S2 cells (data not shown). To confirm a potential physiological significance of Hbs colocalization and binding to Psn, we examined the subcellular distribution of Psn in *hbs* mutant clones. Relative to wild-type cells (marked in red, Figures 6J–6K), Psn accumulated in *hbs* mutant cells (Figures 6J–6K), suggesting that Psn processing or maturation might be affected. To test this hypothesis we analyzed the levels of processed Psn fragments (Psn is synthesized as an immature holoprotein that exists as two closely linked endoproteolytic fragments [Thinakaran et al., 1996]). In the PsnHA construct the HA-tag is associated with the N-terminal NTF. Strikingly, in *hbs* mutant larvae (hbs^{J5}/*Df*), there is a marked reduction in Psn-NTF as compared to wild-type control (Figures 6L–6L'). These data suggest that Hbs affects Psn processing, which results in a reduction of active, cleaved Psn in *hbs* mutant cells.

Hbs Genetically Interacts with *Drosophila* APPL

Another well-studied cleavage substrate of Psn is APP (De Strooper et al., 1998; Thinakaran and Koo, 2008). Similar to Notch, APP also undergoes several cleavages, one of which (mediated by Psn) leads to the generation of amyloid-β peptide, a major component of the neurotoxic plaques found in Alzheimer's disease patients (Goate et al., 1991; Thinakaran et al., 1996). Amyloid-β peptide is generated by sequential cleavage of APP by β-secretase followed by γ-secratase. In *Drosophila*, an APP-related protein (Appl) has been identified (Rosen et al., 1989). Intriguingly, one report suggests that Appl behaves in a similar manner to mammalian APP in that it can aggregate, forming toxic amyloid deposits in neurons (Carmine-Simmen et al., 2009). As our data suggest that Hbs is required for the activity of Psn and *Drosophila* Appl is processed by Psn in the same way as its mammalian ortholog, we tested whether Hbs can affect the function of *Drosophila* Appl. Strikingly, knockdown of *appl* in the eye (*sevGal4 > UAS-appl-IR*) resulted in PCP-like phenotypes (besides loss of photoreceptors), characterized by the presence of R3-R3 symmetrical clusters (Figure 7B). Coexpression of *hbs-IR* with *appl-IR* (*sevgal4 > UAS-appl-IR, UAS-hbsIR*) significantly enhanced the *appl-IR* PCP phenotype (Figures 7C and 7D), arguing for a role of Hbs in Appl function. To test whether Hbs affected processing of Appl via Psn, we used an established Appl-reporter (Loewer et al., 2004; Figure S6), which provides a direct readout of Psn-mediated cleavage of Appl-ICD (AICD) at the membrane, by activating GFP transcription, and thus this effect can be quantified. The fusion reporter construct is under Gal4/UAS control and thus can be expressed in a tissue specific manner. Expression of the reporter alone in developing eyes (*sevGal4 > UAS-AppLV-GFP*) yields a GFP signal because of endogenous Psn-mediated processing in photoreceptor cells (Figure 7E). Strikingly, expression of *hbs-IR* (under *sevGal4*) markedly suppresses the cleavage of this fusion protein, resulting in a significant reduction of GFP (Figures 7F–7G). These data establish that Hbs is generally required for Psn-mediated cleavages, as it affects both N and Appl functions and corroborates our conclusion that Hbs is required/important for the stability or cleavage of Psn.

DISCUSSION

In this study we have identified the IgSF member Hbs/Nephrin as a positive regulator of Psn processing, thus affecting N signaling and Appl function. Previous work has primarily defined a role for Hbs/Neprhins in heterophyllic cell-cell adhesion contexts, including podocyte function in mammalian kidneys (Kawachi et al., 2006), muscle cell fusion and morphogenesis in *Drosophila*, and the organization of interommatidial precursor cells (IPCs) in late pupal eye patterning in *Drosophila* (Artero et al., 2001; Bao and Cagan, 2005; Shelton et al., 2009). Here, we show that Hbs physically associates with Psn and is required for its processing and/or stability. In *hbs* mutant tissue, Psn-mediated cleavage and subsequent N signaling is compromised. In addition to N, Psn cleaves Amyloid precursor protein (APP) to generate beta amyloid (Aβ) peptides, the primary components of amyloid plaques implicated in Alzheimer's disease (De Strooper, 2003; Thinakaran et al., 1996). Accordingly, Hbs also affects the cleavage of the *Drosophila* Amyloid precursor protein-like (Appl) protein. It is likely that the intracellular region of Hbs is acting in the Psn-associated function as a hbs mutant allele causing a truncation of the intracellular region, hbs459, shows similar N-signaling-associated phenotypes as the general Hbs knockdown, Mpreover, we did not detect a requirement for the

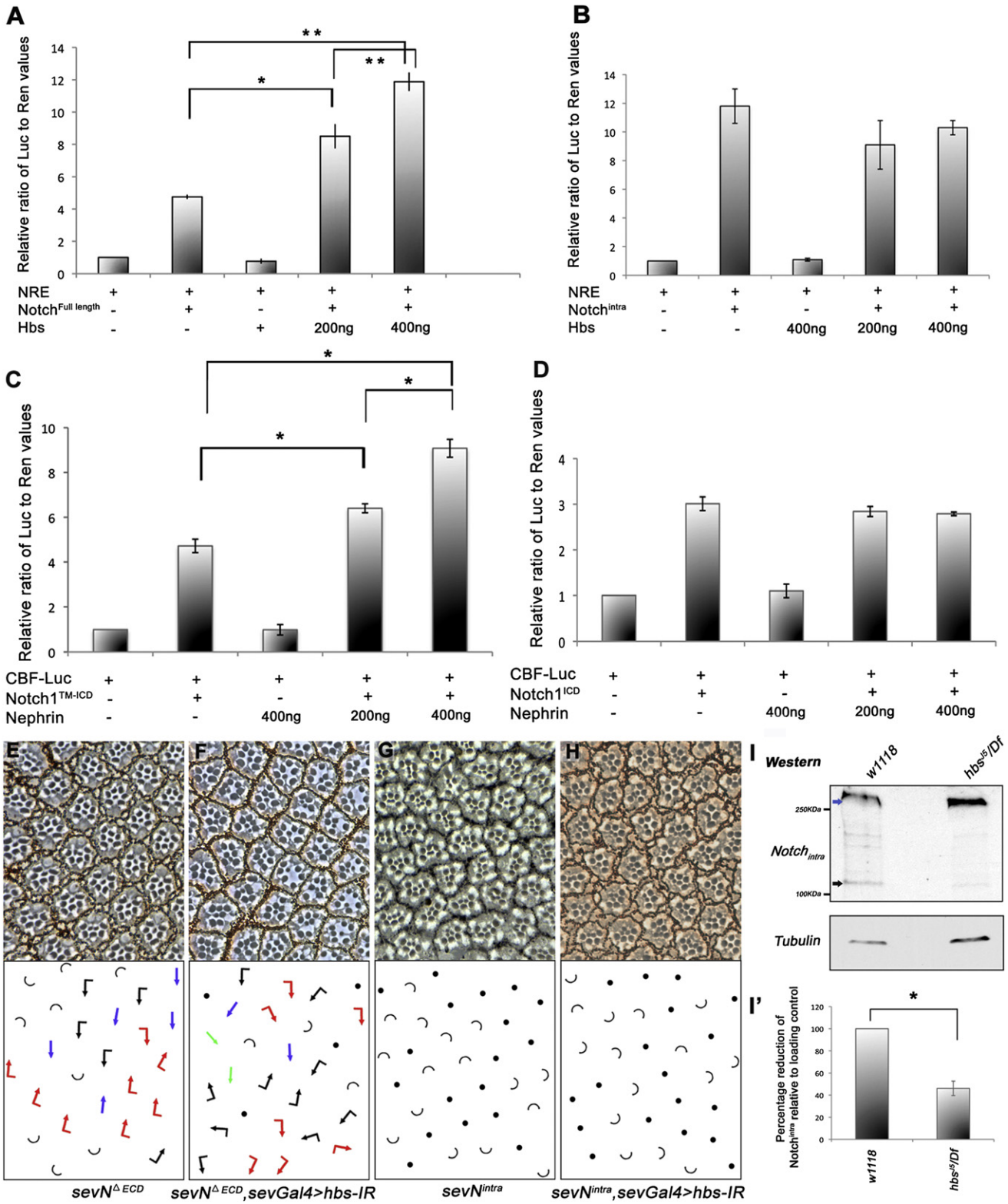

Figure 5. *hbs* Is Required for the Activity of Membrane-Tethered Notch

(A and B) Activation of N signaling induced luciferase reporter containing Su(H) binding sites (NREs) in S2 cells cotransfected with Hbs along with either full-length N (A) or N^{ICD} (B). Hbs expression causes an increase in activity of full-length N in a dose-dependent manner, whereas reporter activity induced by intracellular N^{ICD} remains unaffected by Hbs. Values represent mean ratio of luciferase/renilla control (internal control). Representative experiment from three independent experiments is shown (error bars represent standard deviations within each experiment). p values were *$p < 0.05$ and **$p < 0.005$ (Student's t test).

cell-adhesion binding partners of Hbs, Roughest and Kirre (the *Drosophila* Neph orthologs), in N signaling (data not shown), again suggesting that Hbs/Nephrin regulation of N signaling is independent of its role in cell adhesion.

Hbs and γ-Secretase Complex Function

Regulated membrane proteolysis is important for many signaling pathways. γ-secretase is a large multiprotein complex, whose function is to catalyze cleavage of type I membrane proteins, including the well-studied N receptor and APP. The γ-secretase complex is 220 kDa protein complex, consisting of Psn, Nct, APH-1 (anterior pharynx defective), and PEN-2 (presenilin enhancer 2). Psn constitutes the catalytic subunit of the complex, whereas Nct has been suggested to function in substrate recognition and Psn stability (Chung and Struhl, 2001; De Strooper and Annaert, 2010; Hu et al., 2002; López-Schier and St Johnston, 2002; Struhl and Greenwald, 1999). Our study highlights the role of Hbs in N and Appl in *Drosophila* by affecting Psn maturation, but whether mammalian Nephrin can also affect APP or other type I membrane protein cleavage remains unknown.

What is the function of Hbs in the γ-secretase complex? Nct, Aph-1, and Pen-2 have been shown to affect the stability of Psn (López-Schier and St Johnston, 2002). Hbs also appears to be required for the proper maturation and/or stability of Psn (Figures 6J–6L). We did not see a change in Notch expression levels in *hbs* loss-of-function scenarios (e.g., when *hbs-IR* was expressed in the posterior compartment), suggesting that Hbs acts on Psn rather than N and/or Appl. Furthermore, colocalization of Psn and Hbs in imaginal discs suggests that Hbs and Psn are present in the same subcellular vesicular compartment(s). This is consistent with previous studies, showing that most of Psn inside cells accumulates in ER and vesicular structures (Hu et al., 2002). Significant amounts of Hbs are present in intracellular puncta, and this pool of Hbs might affect Psn processing or stability, possibly in conjunction with other γ-secretase components. Thus, Hbs is likely to affect N and Appl cleavage via its effect on Psn.

Experiments in *Drosophila* suggest that overexpression of Hbs gives similar phenotypes to *hbs* loss of function. One possibility to explain this conundrum could be that overexpression of Hbs acts as a dominant negative. Indeed removing a genomic copy of *hbs* in the Hbs overexpression background enhances its phenotype (data not shown), consistent with this model. This is similarly consistent with existing data for Psn: overexpression of Psn causes similar phenotypes as *psn* loss of function (Ye and Fortini, 1999). It has been hypothesized that overexpression of Psn forms insoluble complexes that downregulate signaling. Indeed, several studies have highlighted that all four components of the γ-secretase complex have to be expressed for it to be active (Edbauer et al., 2003; Stempfle et al., 2010). Thus, it is likely that an excess of one component of the complex renders it less active. These results are consistent with and support our hypothesis that Hbs behaves in a similar manner to components of the γ-secratase complex that are important for Psn processing.

Transcriptional Regulation of *hbs* Expression

In contrast to Nct and Psn, which appear to be uniformly expressed in *Drosophila* (Nowotny et al., 2000; Ye and Fortini, 1998), *hbs* expression is highly regulated and under the control of several signaling pathways in different tissues (although *hbs* is also expressed constitutively at low levels in all cells). As such, different endogenous levels of Hbs could affect the stability/processing of Psn and the γ-secretase complex, boosting its activity where needed. This is notion consistent with the expression pattern of *hbs*, which is upregulated where N signaling is highest, for example, at the wing margin (via Wg-signaling, Figure S3) or during eye development in ommatidial preclusters (likely via Egfr/Ras signaling, data not shown). In developing embryos, *hbs* expression is regulated via N and Ras signaling (Artero et al., 2001). As increased *hbs* expression correlates with cells that require high N-signaling levels (wing margin, SOP clusters [Figure S1], or ommatidial preclusters), *hbs* might integrate input from several signaling pathways to modulate Psn activity and hence N-signaling levels.

Nephrins and Notch Signaling

In mammalian cells, coexpression of Nephrin resulted in increased Notch reporter activity (Figures 5C and 5D) when the membrane-tethered form of Notch was expressed, whereas soluble Notch^{intra} was not affected. This behavior was very similar to the equivalent experiments in *Drosophila* S2 cells and in vivo. Thus, there is a likely mechanistic conservation of Hbs and Nephrin function to regulate N-signaling activity via the γ–secretase complex. In mammals, like in *Drosophila*, most studies related to Nephrin family members have focused on their role in cell adhesion with a focus on the kidney. In kidney podocytes, Nephrin has been studied extensively in the context of the

(C and D) Activation of mammalian CBF Notch luciferase reporter in 293T cells cotransfected with Nephrin along with either mN1^{TM-ICD} (C) or mN1^{ICD} (D); coexpression of Nephrin-enhanced mN1^{TM-ICD}-based CBF reporter activation in a dose-dependent manner (*$p < 0.005$), whereas mN1^{ICD}-mediated reporter induction remained unchanged. Error bars denote standard deviations within each experiment.

(E–H) Tangential sections of adult eyes of indicated genotypes; anterior is left and dorsal up. Arrows are as in Figure 1, with blue arrows representing R4-R4 type symmetrical clusters and half circles ommatidia with >1 R7 (at the expense of R1/R6, as frequently observed in N overactivation caused by transformation of R1 and/or R6 to R7; Fortini et al., 1993; Tomlinson and Struhl, 1999).

(E and F) Knockdown of *hbs* (*sevGal4 > hbs-IR*) markedly suppresses the phenotype of membrane-tethered *sevN$^{\Delta ECD}$* (compare E and F; note even some R3-R3-type clusters; quantified in Figure S4).

(G and H) The effect of "active" cytoplasmic *sev-N^{intra}* (G) is not affected by *hbs-IR* (H), suggesting a requirement of Hbs at the membrane.

(I and I') Western blot of third instar larval eye-brain complexes showing cleavage pattern of endogenous N protein. In wild-type larvae higher molecular weight full-length N (blue arrow) and smaller cleavage products, N-intra-fragments (~120 K, black arrow) are detected. In samples from *hbs* mutants, there is a significant reduction in the levels of N cleavage fragments, whereas levels of full-length N protein are unchanged (γ-Tubulin, bottom, serves as loading control). (I') Quantification showing percentage reduction of Notch^{intra} cleavage products (black arrows), which are reduced in *hbs* mutant larval eye-brain complexes (error bars represent standard deviations with *$p < 0.01$).

See also Figure S4.

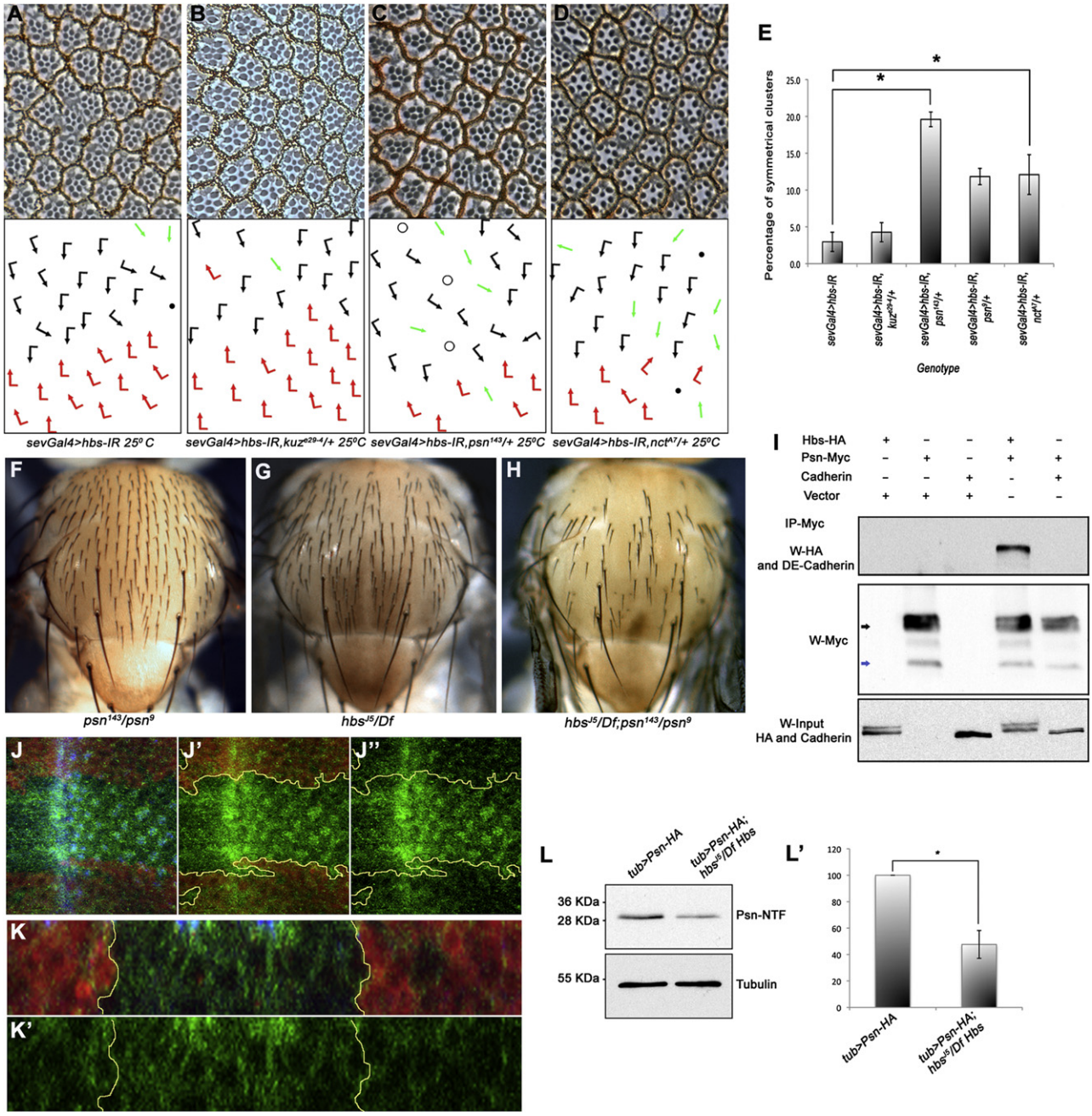

Figure 6. Hbs Is Required for Psn Function and Processing

(A–D) Tangential adult eye sections of indicated genotypes; anterior is left and dorsal up (arrows and dots as in Figure 1). *sevGal4 > hbs-IR* (A) is not affected by *kuz*$^{e29\text{-}4/+}$ heterozygosity (B), whereas dosage reduction of *psn* (*sevGal4 > hbs-IR, psn*^{143}/+) (C) and *nct* (*sevGal4 > hbs-IR, nct*^{A7}/+) (D) strongly enhances the *hbs-IR* phenotypes, suggesting a positive relationship between Psn and Hbs.

(E) Quantification of R3-R3 symmetrical clusters in genotypes shown in (B)–(D). Error bars represent standard deviations (**p < 0.001).

(F–H) Adult nota of genotypes indicated; anterior is up. (F) heteroallelic hypomorphic *psn*^{143}/*psn*^{9} combination with normal mechanosensory bristle arrangement; (G) *hbs*$^{\Delta 5}$/*Df(2R)ED2423* mutant thorax displaying occasional "bald" patches as a result of missing bristles; and (H) *hbs*$^{\Delta 5}$/*Df(2R)ED2423; psn*^{143}/*psn*^{9} double mutant thorax with many bristles missing, suggesting synergistic interaction and *hbs* and *psn* acting in the same molecular context.

(I) Hbs is coimmunoprecipated (co-IP) by Psn: immunoblot from S2 cell whole cell lysates expressing Hbs-HA, either alone or in combination with Psn-Myc or DE-cadherin (acting as negative control). Cell lysates were immunoprecipitated with anti-Myc (IP-Myc), and blots were probed with anti-HA (Hbs) and anti-DE-cadherin antibodies, revealing specific Co-IP of Hbs with Psn, whereas DE-cadherin (a control protein similar to Hbs) does not bind to Psn-Myc (bottom: Hbs input). See also Figure S5I for additional controls.

(J–J") Confocal projections of third instar larval eye discs stained for Psn-HA (green), DE-cadherin (blue, labeling apical surfaces of all cells), and lacZ (red, marking wild-type tissue: *hbs* mutant tissue marked by absence of red; outlined by yellow lines in J' and J"). *hbs* mutant tissue shows marked accumulation of PsnHA.

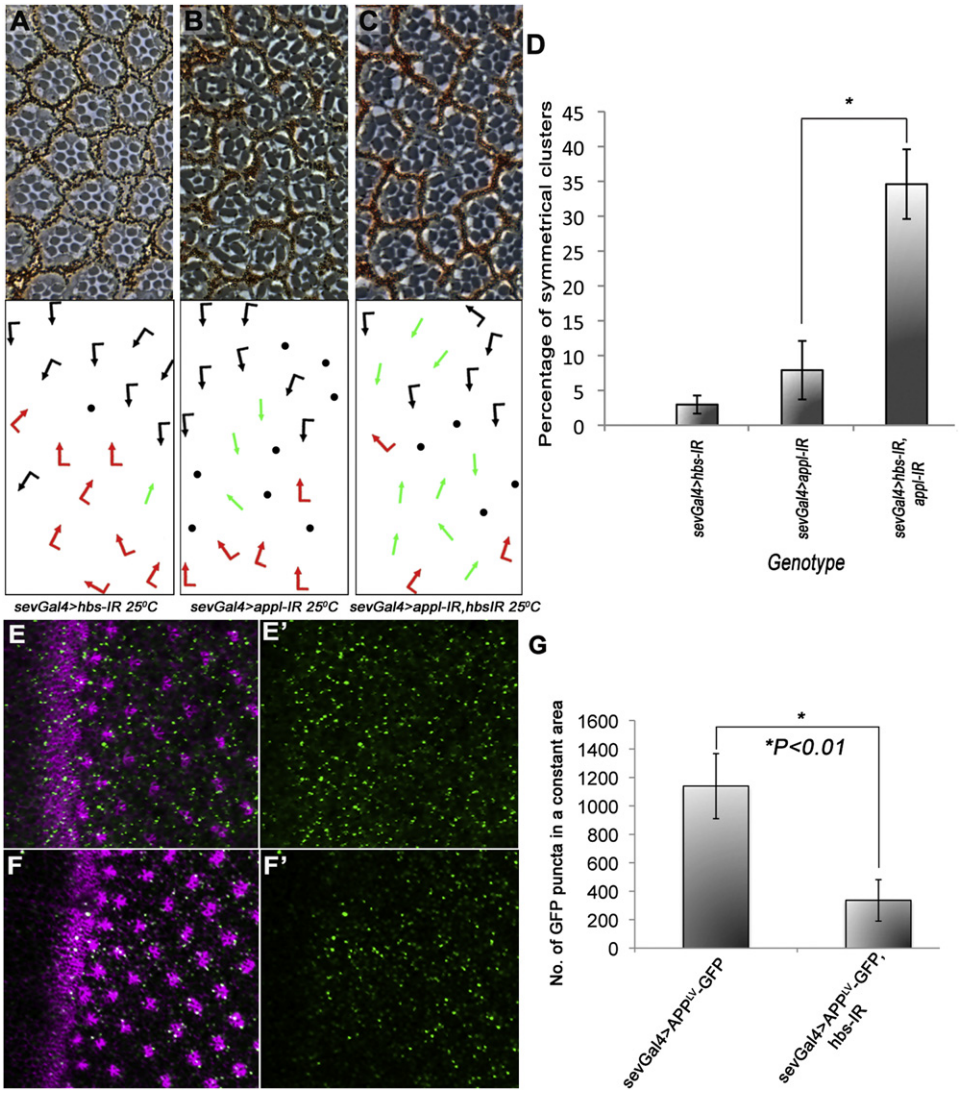

Figure 7. *hbs* Genetically Interacts with *dAppl*

(A–C) Tangential sections of adult eyes of indicated genotypes; anterior is left and dorsal up. (A) *sevGal4*, *UAS-hbs-IR* eye at 25°C, with phenotypes as seen previously (e.g., Figure 1B), and (B) *sevGal4*, *UAS-appl-IR* eye at 25°C. Note several ommatidia that adopt R3-R3 type symmetrical arrangement. (C) *sevGal4*, *UAS-appl-IR, UAS-hbs-IR* at 25°C. Note enhancement of either individual RNAi phenotype, indicating a positive (synergistic) relationship between Appl and Hbs. (D) Quantification of R3-R3 symmetrical clusters in the genotypes shown in (A–C). Error bars represent standard deviations (*p < 0.01).

(E–G) Confocal projections of third instar larval eye discs expressing the APPLV-GFP fusion protein under the control of *sevGal4* (*sevGal4* > *AppLV-GFP*) showing expression of GFP behind the MF and its quantification (G). Expression of the GFP reporter is significantly reduced in eye discs coexpressing *hbs-IR* (*sevGal4* > *AppLV-GFP, UAS-hbsIR*), indicating that there is reduction of APPL-ICD membrane cleavage when Hbs is compromised (F). Error bars show standard deviations, with *p < 0.01 in (G). See also Figure S6F for schematic of reporter assay. See also Figure S6.

slit diaphragm, involved in filtering blood (Holzman et al., 1999; Ruotsalainen et al., 1999). Mutations in Nephrin are associated with congenital nephritic syndrome of the Finnish-type (Kallinen et al., 2001; Koziell et al., 2002). Our study supports the idea that Nephrin family members play important roles in other tissues. This is consistent with a recent report in which Nephrin has been shown to be involved in cardiac function (Wagner et al., 2011), corroborating the importance of Nephrin in biological contexts in which Notch signaling plays an important role during development.

(K–K'') Transverse (x/z)-section of eye disc shown in (J); note accumulation of Psn in the *hbs* mutant tissue (marked by absence of lacZ).

(L and L') Western blot of third instar larval eye-brain complexes showing Psn-NTF fragment in wild-type and *hbs* mutant larvae. In *hbs* mutant larvae there is a marked reduction of Psn-NTF fragment (quantified in L') as compared to control flies (γ-Tubulin, bottom, serves as loading control). Error bars represent standard deviations, with *p < 0.001.

See also Figure S5.

EXPERIMENTAL PROCEDURES

Drosophila Stocks

Fly crosses were grown on standard food at 25°C unless otherwise stated. The following stocks were used and sources are as indicated:

sevGal4; *tubGal4*; *mδ*$^{0.5}$*Gal4, UAS-GFP*; *enGal4*; *pnrGal4*, *hs-FLP*; *actin > y > Gal4*, *UAS-GFP*; *Rab5GFP*; *Rab11GFP*; and *Rab7GFP* are our lab stocks;
UAS-Hbs, *hbsLacZ*, and *hbs*^{459} (R. Cagan);
tub > PsnHA (G. Struhl);
nct^{A7}, *sevN*^{intra} and *sevN*$^{\Delta ECD}$ (Mark Fortini);
UAS-hbs-IR and *UAS-wg-IR* were from the Vienna *Drosophila* RNAi Center;
Df(2R)ED2423, hbs^{EP}, *N*^{55e11}, *psn*^{143}, *psn*^{9}, *UAS-appl-IR* (stock no. 28043), *UAS-dicer2*, *kuz*$^{e29-4}$ and *w1118*; *P{w[+mc]-UAS-mycAPP.LV}* (II) were from the Bloomington stock center.

hbs^{I5} was generated using a FLP-recombinase-mediated excision of two *piggyBac/FRT* insertions (PBac{RB}e04215 and PBac{WH}f04302) as previously described (Parks et al., 2004).

Immunofluorescence and Histology

Third instar larvae or 24-hr-old white pupae were dissected in ice-cold PBS and fixed in 4% paraformaldehyde for 20 min. After washing in PBT (PBS + 0.1% Triton), discs were incubated in primary antibody overnight at 4°C followed by washes in PBT, secondary antibody incubation for 2 hr, and washes again in PBT, and they were subsequently mounted in Mowiol. The following primary antibodies were used: mouse anti-Cut, rat anti-DE cadherin, rat anti-Elav (DSHB), rabbit anti-Hbs (gift from Karl Fischbach), and anti-GFP (Molecular Probes, Grand Island, NY, USA).

S2 cells were grown on coverslips placed in 6-well plates containing Schneider's *Drosophila* medium (GIBCO, Invitrogen, Carlsbad, CA, USA) supplemented with 10% FBS and antibiotics. Immunofluorescence cells were washed in PBS, fixed in 4% paraformaldehyde for 20 min at room temperature (RT), permeabilized in PBT (0.1% Triton X-100 in PBS) for 10 min, and "blocked" with 0.1% BSA in PBS. Cells were then incubated with mouse anti-Myc and rat anti-HA antibodies (Santa Cruz Biotechnology, Santa Cruz, CA, USA, and Roche, Indianapolis, IN, USA) overnight at 4°C, followed by washes with PBS. Cells were then incubated with secondary antibodies and Hoechst dye (to stain nuclei) for 2 hr at room temperature, followed by washes in PBS, and mounted in Vectashield (Vector Labs, Burlingame, CA, USA).

Western Blotting and Coimmunoprecipitation

For coimmunoprecipitation experiments, S2 cells were transfected with Hbs-HA and/or Psn-Myc (gift from Mark Fortini) or Fz-Myc using Effectene (QIAGEN, Hilden, Germany) in accordance with the manufacturer's instructions. Cells were harvested after 48 hr, washed, and lysed in ice-cold lysis buffer (50 mM Tris-HCl [pH 8.0], 150 mM NaCl, 1 mM EDTA, 5 mM β-glycerophosphate, protease inhibitor cocktail I and II [Sigma-Aldrich, St. Louis, MO, USA], and 1% Triton X-100). Lysed samples were immunoprecipitated using mouse anti-Myc (9E10, Santa Cruz Biotechnology) overnight at 4°C and later protein-antibody complexes were pulled down using Protein G Agarose. Beads were washed in lysis buffers, and western blots were carried out with immunoprecipitated samples using rat anti-HA, mouse anti-γ-Tubulin,or mouse anti-Myc antibodies.

For in vivo Notch cleavage analyses, five larval eye/brain complexes were lysed in ice-cold hypotonic lysis buffer (10 mM KCl, 20 mM Tris [pH 7.5], 0.1% mercaptoethanol, and 1 mM EDTA, along with protease and phosphatase inhibitors [Sigma-Aldrich]). Supernatant from these extracts were resolved and subjected to standard western blotting procedures using mouse anti-Notch^{intra} (DSHB, 1:500) and mouse anti-γ-tubulin (Sigma-Aldrich, 1:1,000) antibodies.

Notch Reporter Assays

S2 cells were transfected with N-responsive Su(H) sites NRE plasmid (gift from Sarah Bray), together with pMTNotch$^{Full\ length}$ or pMTNotch^{intra} (from DGRC), either alone or along with varying conc. of Hbs (200 and 400 ng). Renilla-expressing plasmid was cotransfected as an internal control. N-constructs were induced with 600 μM $CuSO_4$ 24 hr after transfection for 18 hr. Cells were then lysed, and luciferase activity was measured using the Dual-Luciferase Reporter Assay System (Promega, Madison, WI, USA). Reporter activity was calculated via the luciferase/renilla values. In mammalian 293T cells, CBF reporter (gift from Reshma Taneja) was cotransfected with Nephrin (gift from Christan Faul) along with either mNT$^{M\text{-}ICD}$ or mN^{ICD}. Cells were lysed 48 hr after transfection, and luciferase activity was monitored as described previously.

SUPPLEMENTAL INFORMATION

Supplemental Information includes six figures and can be found with this article online at http://dx.doi.org/10.1016/j.devcel.2012.04.021.

ACKNOWLEDGMENTS

We thank the Bloomington Stock Center, Developmental Studies Hybridoma Bank, Spyros Artavanis-Tsakonas, Sujin Bao, Sarah Bray, Ross Cagan, Mark Fortini, Christian Faul, Edward Giniger, Gary Struhl, and Reshma Taneja for various fly stocks, plasmid DNAs, and antibodies, as well as all Mlodzik laboratory members for helpful suggestions and discussion. We are most grateful to Karl Fischbach for a gift of the limited Hbs antibody. We thank Mark Fortini, William Gault, Edward Giniger, Ruth Johnson, Lindsay Kelly, and Robert Krauss for helpful comments on drafts of the manuscript and Aurore Dussert, Susanna Franks, Joyce Lau, and Sophy Okello for technical help. Confocal laser microscopy was performed at the MSSM Microscopy SRF. This research was supported by a National Institutes of Health grant to M.M.

Received: October 25, 2011
Revised: March 13, 2012
Accepted: April 30, 2012
Published online: July 16, 2012

REFERENCES

Artavanis-Tsakonas, S., and Muskavitch, M.A. (2010). Notch: the past, the present, and the future. Curr. Top. Dev. Biol. *92*, 1–29.

Artero, R.D., Castanon, I., and Baylies, M.K. (2001). The immunoglobulin-like protein Hibris functions as a dose-dependent regulator of myoblast fusion and is differentially controlled by Ras and Notch signaling. Development *128*, 4251–4264.

Bao, S., and Cagan, R. (2005). Preferential adhesion mediated by Hibris and Roughest regulates morphogenesis and patterning in the Drosophila eye. Dev. Cell *8*, 925–935.

Boutros, M., Paricio, N., Strutt, D.I., and Mlodzik, M. (1998). Dishevelled activates JNK and discriminates between JNK pathways in planar polarity and wingless signaling. Cell *94*, 109–118.

Bray, S., Musisi, H., and Bienz, M. (2005). Bre1 is required for Notch signaling and histone modification. Dev. Cell *8*, 279–286.

Carmine-Simmen, K., Proctor, T., Tschäpe, J., Poeck, B., Triphan, T., Strauss, R., and Kretzschmar, D. (2009). Neurotoxic effects induced by the Drosophila amyloid-beta peptide suggest a conserved toxic function. Neurobiol. Dis. *33*, 274–281.

Chung, H.M., and Struhl, G. (2001). Nicastrin is required for Presenilin-mediated transmembrane cleavage in Drosophila. Nat. Cell Biol. *3*, 1129–1132.

Cooper, M.T., and Bray, S.J. (1999). Frizzled regulation of Notch signalling polarizes cell fate in the Drosophila eye. Nature *397*, 526–530.

de Celis, J.F., Garcia-Bellido, A., and Bray, S.J. (1996). Activation and function of Notch at the dorsal-ventral boundary of the wing imaginal disc. Development *122*, 359–369.

De Strooper, B. (2003). Aph-1, Pen-2, and Nicastrin with Presenilin generate an active gamma-Secretase complex. Neuron *38*, 9–12.

De Strooper, B., and Annaert, W. (2010). Novel research horizons for presenilins and γ-secretases in cell biology and disease. Annu. Rev. Cell Dev. Biol. *26*, 235–260.

De Strooper, B., Annaert, W., Cupers, P., Saftig, P., Craessaerts, K., Mumm, J.S., Schroeter, E.H., Schrijvers, V., Wolfe, M.S., Ray, W.J., et al. (1999). A presenilin-1-dependent gamma-secretase-like protease mediates release of Notch intracellular domain. Nature *398*, 518–522.

De Strooper, B., Saftig, P., Craessaerts, K., Vanderstichele, H., Guhde, G., Annaert, W., Von Figura, K., and Van Leuven, F. (1998). Deficiency of presenilin-1 inhibits the normal cleavage of amyloid precursor protein. Nature *391*, 387–390.

del Alamo, D., and Mlodzik, M. (2006). Frizzled/PCP-dependent asymmetric neuralized expression determines R3/R4 fates in the Drosophila eye. Dev. Cell *11*, 887–894.

Dworak, H.A., Charles, M.A., Pellerano, L.B., and Sink, H. (2001). Characterization of Drosophila hibris, a gene related to human nephrin. Development *128*, 4265–4276.

Edbauer, D., Winkler, E., Regula, J.T., Pesold, B., Steiner, H., and Haass, C. (2003). Reconstitution of gamma-secretase activity. Nat. Cell Biol. *5*, 486–488.

Fanto, M., and Mlodzik, M. (1999). Asymmetric Notch activation specifies photoreceptors R3 and R4 and planar polarity in the Drosophila eye. Nature *397*, 523–526.

Fehon, R.G., Kooh, P.J., Rebay, I., Regan, C.L., Xu, T., Muskavitch, M.A., and Artavanis-Tsakonas, S. (1990). Molecular interactions between the protein products of the neurogenic loci Notch and Delta, two EGF-homologous genes in Drosophila. Cell *61*, 523–534.

Fortini, M.E. (2009). Notch signaling: the core pathway and its posttranslational regulation. Dev. Cell *16*, 633–647.

Fortini, M.E., and Artavanis-Tsakonas, S. (1994). The suppressor of hairless protein participates in notch receptor signaling. Cell *79*, 273–282.

Fortini, M.E., Rebay, I., Caron, L.A., and Artavanis-Tsakonas, S. (1993). An activated Notch receptor blocks cell-fate commitment in the developing Drosophila eye. Nature *365*, 555–557.

Goate, A., Chartier-Harlin, M.C., Mullan, M., Brown, J., Crawford, F., Fidani, L., Giuffra, L., Haynes, A., Irving, N., James, L., et al. (1991). Segregation of a missense mutation in the amyloid precursor protein gene with familial Alzheimer's disease. Nature *349*, 704–706.

Hartmann, D., de Strooper, B., Serneels, L., Craessaerts, K., Herreman, A., Annaert, W., Umans, L., Lübke, T., Lena Illert, A., von Figura, K., and Saftig, P. (2002). The disintegrin/metalloprotease ADAM 10 is essential for Notch signalling but not for alpha-secretase activity in fibroblasts. Hum. Mol. Genet. *11*, 2615–2624.

Holzman, L.B., St John, P.L., Kovari, I.A., Verma, R., Holthofer, H., and Abrahamson, D.R. (1999). Nephrin localizes to the slit pore of the glomerular epithelial cell. Kidney Int. *56*, 1481–1491.

Hu, Y., and Fortini, M.E. (2003). Different cofactor activities in gamma-secretase assembly: evidence for a nicastrin-Aph-1 subcomplex. J. Cell Biol. *161*, 685–690.

Hu, Y., Ye, Y., and Fortini, M.E. (2002). Nicastrin is required for gamma-secretase cleavage of the Drosophila Notch receptor. Dev. Cell *2*, 69–78.

Kallinen, J., Heinonen, S., Ryynänen, M., Pulkkinen, L., and Mannermaa, A. (2001). Antenatal genetic screening for congenital nephrosis. Prenat. Diagn. *21*, 81–84.

Kawachi, H., Miyauchi, N., Suzuki, K., Han, G.D., Orikasa, M., and Shimizu, F. (2006). Role of podocyte slit diaphragm as a filtration barrier. Nephrology (Carlton) *11*, 274–281.

Kopan, R., and Ilagan, M.X. (2009). The canonical Notch signaling pathway: unfolding the activation mechanism. Cell *137*, 216–233.

Koziell, A., Grech, V., Hussain, S., Lee, G., Lenkkeri, U., Tryggvason, K., and Scambler, P. (2002). Genotype/phenotype correlations of NPHS1 and NPHS2 mutations in nephrotic syndrome advocate a functional inter-relationship in glomerular filtration. Hum. Mol. Genet. *11*, 379–388.

Lai, E.C., and Orgogozo, V. (2004). A hidden program in Drosophila peripheral neurogenesis revealed: fundamental principles underlying sensory organ diversity. Dev. Biol. *269*, 1–17.

Loewer, A., Soba, P., Beyreuther, K., Paro, R., and Merdes, G. (2004). Cell-type-specific processing of the amyloid precursor protein by Presenilin during Drosophila development. EMBO Rep. *5*, 405–411.

López-Schier, H., and St Johnston, D. (2002). Drosophila nicastrin is essential for the intramembranous cleavage of notch. Dev. Cell *2*, 79–89.

Mlodzik, M. (1999). Planar polarity in the *Drosophila* eye: a multifaceted view of signaling specificity and cross-talk. EMBO J. *18*, 6873–6879.

Mumm, J.S., and Kopan, R. (2000). Notch signaling: from the outside in. Dev. Biol. *228*, 151–165.

Muñoz-Soriano, V., Belacortu, Y., Durupt, F.C., Muñoz-Descalzo, S., and Paricio, N. (2011). Mtl interacts with members of Egfr signaling and cell adhesion genes in the Drosophila eye. Fly (Austin) *5*, 88–101.

Naruse, S., Thinakaran, G., Luo, J.J., Kusiak, J.W., Tomita, T., Iwatsubo, T., Qian, X., Ginty, D.D., Price, D.L., Borchelt, D.R., et al. (1998). Effects of PS1 deficiency on membrane protein trafficking in neurons. Neuron *21*, 1213–1221.

Nowotny, P., Gorski, S.M., Han, S.W., Philips, K., Ray, W.J., Nowotny, V., Jones, C.J., Clark, R.F., Cagan, R.L., and Goate, A.M. (2000). Posttranslational modification and plasma membrane localization of the Drosophila melanogaster presenilin. Mol. Cell. Neurosci. *15*, 88–98.

Pan, D., and Rubin, G.M. (1997). Kuzbanian controls proteolytic processing of Notch and mediates lateral inhibition during Drosophila and vertebrate neurogenesis. Cell *90*, 271–280.

Parks, A.L., Cook, K.R., Belvin, M., Dompe, N.A., Fawcett, R., Huppert, K., Tan, L.R., Winter, C.G., Bogart, K.P., Deal, J.E., et al. (2004). Systematic generation of high-resolution deletion coverage of the Drosophila melanogaster genome. Nat. Genet. *36*, 288–292.

Ray, W.J., Yao, M., Nowotny, P., Mumm, J., Zhang, W., Wu, J.Y., Kopan, R., and Goate, A.M. (1999). Evidence for a physical interaction between presenilin and Notch. Proc. Natl. Acad. Sci. USA *96*, 3263–3268.

Rosen, D.R., Martin-Morris, L., Luo, L.Q., and White, K. (1989). A Drosophila gene encoding a protein resembling the human beta-amyloid protein precursor. Proc. Natl. Acad. Sci. USA *86*, 2478–2482.

Ruotsalainen, V., Ljungberg, P., Wartiovaara, J., Lenkkeri, U., Kestilä, M., Jalanko, H., Holmberg, C., and Tryggvason, K. (1999). Nephrin is specifically located at the slit diaphragm of glomerular podocytes. Proc. Natl. Acad. Sci. USA *96*, 7962–7967.

Schroeter, E.H., Kisslinger, J.A., and Kopan, R. (1998). Notch-1 signalling requires ligand-induced proteolytic release of intracellular domain. Nature *393*, 382–386.

Selkoe, D., and Kopan, R. (2003). Notch and Presenilin: regulated intramembrane proteolysis links development and degeneration. Annu. Rev. Neurosci. *26*, 565–597.

Shellenbarger, D.L., and Mohler, J.D. (1978). Temperature-sensitive periods and autonomy of pleiotropic effects of l(1)Nts1, a conditional notch lethal in Drosophila. Dev. Biol. *62*, 432–446.

Shelton, C., Kocherlakota, K.S., Zhuang, S., and Abmayr, S.M. (2009). The immunoglobulin superfamily member Hbs functions redundantly with Sns in interactions between founder and fusion-competent myoblasts. Development *136*, 1159–1168.

Sotillos, S., Roch, F., and Campuzano, S. (1997). The metalloprotease-disintegrin Kuzbanian participates in Notch activation during growth and patterning of Drosophila imaginal discs. Development *124*, 4769–4779.

Stempfle, D., Kanwar, R., Loewer, A., Fortini, M.E., and Merdes, G. (2010). In vivo reconstitution of gamma-secretase in Drosophila results in substrate specificity. Mol. Cell. Biol. *30*, 3165–3175.

Struhl, G., and Adachi, A. (1998). Nuclear access and action of notch in vivo. Cell *93*, 649–660.

Struhl, G., and Greenwald, I. (1999). Presenilin is required for activity and nuclear access of Notch in Drosophila. Nature *398*, 522–525.

Strutt, H., and Strutt, D. (1999). Polarity determination in the Drosophila eye. Curr. Opin. Genet. Dev. *9*, 442–446.

Thinakaran, G., Borchelt, D.R., Lee, M.K., Slunt, H.H., Spitzer, L., Kim, G., Ratovitsky, T., Davenport, F., Nordstedt, C., Seeger, M., et al. (1996).

Endoproteolysis of presenilin 1 and accumulation of processed derivatives in vivo. Neuron *17*, 181–190.

Thinakaran, G., and Koo, E.H. (2008). Amyloid precursor protein trafficking, processing, and function. J. Biol. Chem. *283*, 29615–29619.

Tomlinson, A., and Struhl, G. (1999). Decoding vectorial information from a gradient: sequential roles of the receptors Frizzled and Notch in establishing planar polarity in the Drosophila eye. Development *126*, 5725–5738.

Wagner, N., Morrison, H., Pagnotta, S., Michiels, J.F., Schwab, Y., Tryggvason, K., Schedl, A., and Wagner, K.D. (2011). The podocyte protein nephrin is required for cardiac vessel formation. Hum. Mol. Genet. *20*, 2182–2194.

Wen, C., Metzstein, M.M., and Greenwald, I. (1997). SUP-17, a Caenorhabditis elegans ADAM protein related to Drosophila KUZBANIAN, and its role in LIN-12/NOTCH signalling. Development *124*, 4759–4767.

Ye, Y., and Fortini, M.E. (1998). Characterization of Drosophila Presenilin and its colocalization with Notch during development. Mech. Dev. *79*, 199–211.

Ye, Y., and Fortini, M.E. (1999). Apoptotic activities of wild-type and Alzheimer's disease-related mutant presenilins in Drosophila melanogaster. J. Cell Biol. *146*, 1351–1364.

Zheng, L., Zhang, J., and Carthew, R.W. (1995). frizzled regulates mirror-symmetric pattern formation in the Drosophila eye. Development *121*, 3045–3055.